Machinability analysis of dry drilling of carbon/epoxy composites: cases of exit delamination and cylindricity error

M. F. Ameur, Malek Habak, M. Kenane, H. Aouici, Mohammed Cheikh

Machinability analysis of dry drilling of carbon/epoxy composites: cases of exit delamination and cylindricity error

M. F. Ameur[1,2] · M. Habak[3] · M. Kenane[1] · H. Aouici[4] · M. Cheikh[5]

Abstract The aim of this work is to define the cutting conditions that allow the dry drilling of carbon fiber reinforced epoxy (CFRE) composite materials taking into consideration the quality of the drilled holes (the exit delamination factor and the cylindricity error) and the optimum combination of drilling parameters. A further aim is to use grey relational analysis to improve the quality of the drilled holes. The machining parameters were measured according to 3^3 full factorial parameter designs (27 experiments with independent process variables). The experiments were carried out under various cutting parameters with different spindle speeds and feed rates. Drilling tests were done using WC carbide, high-speed steel (HSS), and TiN-coated carbide drills. The experiment design was accomplished by application of the statistical analysis of variance (ANOVA). Results show that the thrust force is mainly influenced by the tool materials and the feed rate, which has a strong influence on the exit delamination factor. On the other hand, the spindle speed particularly affects the cylindricity error of the holes. Correlations were established between spindle speed/feed rate and the various machining parameters so as to optimize cutting conditions. These correlations were found by quadratic regression using response surface methodology (RSM). Finally, tests were carried out to check the concordance of experimental results.

Keywords CFRE composites · Response surface methodology · Dry drilling · Cutting parameters · Exit delamination factor · Cylindricity error

✉ M. F. Ameur
faycalameur@gmail.com

[1] Laboratoire des Sciences et Génie des Matériaux, Faculté de Génie Mécanique et Génie des Procédés USTHB, BP 32, El-Alia, Bab Ezzouar, Algeria

[2] Ecole Nationale Supérieure de Technologie, Cité Diplomatique Dergana-Bordj El Kiffan, Alger, Algeria

[3] Laboratoire des Technologies Innovantes (LTI), IUT d'Amiens, Dépt GMP, Université de Picardie Jules Verne, Avenue Facultés Bailly, 80001 Amiens, France

[4] Laboratoire Mécanique et Structures (LMS), Département de Génie Mécanique, FST, Université 08 Mai 1945, Guelma 24000, Algeria

[5] Université de Toulouse, IUT de Figeac, Mines Albi, ICA (Institut Clément Ader), Campus Jarlard, 81013 Albi cedex 09, France

1 Introduction

In industrial fields such as aerospace and aircraft manufacturing, carbon fiber reinforced epoxy (CFRE) composites are used, because of their excellent mechanical properties. Drilling of composite materials is a very common process in the assembly of aeronautic composite structures. However, the machinability of these composites makes it difficult to yield good-quality products.

With regard to the quality characteristics of drilled holes in CFRE, some problems have been encountered, including surface delamination and fiber pullout. With the increasing demand for advanced composite materials, different cutting conditions are required. Delamination is the most common defect when drilling. This is because of the heterogeneity between fibers and matrix [1]. Some studies have concluded that the delamination factor is related to the thrust force when drilling composite materials [2].

Davim et al. [3] presented a correlation between cutting velocity and feed rate with the delamination of carbon fiber reinforced laminate composites. Recently, Tsao[[4] examined the drilling-induced thrust force of a composite polymer (CFRP) material, with a step-core drill, by taking into

consideration the diameter ratio, feed rate, and spindle speed parameters. For the same material, Zitoune et al. [5] improved drilling by using various dimensions of a double cone drill with analysis including cutting force, tool lifetime, chip form, and hole quality. Elsewhere, Li et al. [6] detailed the effect of variable feed rate and lay-up configuration on surface roughness and integrity following the drilling of CFRP composites under chilled air conditions. Gaitonde et al. [7] analyzed the effects of process parameters on delamination under high-speed drilling using CFRP. Rawat et al. conducted similar experiments [8], but with carbon fiber and a different epoxy matrix. With the same carbon/epoxy composite plates, Piquet et al. [9] investigated the effect of drilling with two types of drills, a conventional twist drill and specific cutting tool. Luís Miguel et al. [10] performed drilling tests with different drills, and the resulting delamination extensions were measured by digital-enhanced radiography and evaluated using the computational techniques of image processing and analysis. Capello [11] studied the differences in delamination mechanisms in drilling with and without a support placed below the glass fiber reinforced plastic work piece. Bhatnagar et al. [12] studied the orthogonal cutting of unidirectional carbon fiber reinforced epoxy composite with different fiber orientations. Rajamurugan et al. [13] analyzed delamination in drilling glass fiber reinforced polyester composites. An attempt has been made to develop empirical relationships between the drilling parameters. Khashaba et al. [14] treated the effect of drill pre-wear on the machinability parameters when drilling glass fiber reinforced epoxy composites (GFRE) under different cutting conditions. Linear regression models were developed to correlate the machinability parameters with the drill wear and cutting conditions.

Rubio et al. [15] chose the Taguchi method to identify the best drilling setup of a glass reinforced polyamide. Another approach, based on a combination of Taguchi's techniques and the analysis of variance (ANOVA), was used to investigate the cutting characteristics of CFRP with high-speed steel (HSS) and cemented carbide drills [3]. In other studies, Sardinas et al. [16] used a micro-genetic algorithm and Krishnamoorthy et al. [17] a fuzzy grey method both with the aim of optimizing the drilling process conditions. Gaitonde et al. analyzed the effects of cutting speed, feed rate, and angle point on the delamination factor by generating response surface methodology (RSM) plots models [7].

Although numerous research studies have been carried out on the effects of cutting parameters on delamination during the drilling of CFRP composites, few have been reported on the effect of the geometric quality of the hole [18].

The studies mentioned above discuss the cutting of composite materials, but they make no assumptions about geometric cylindricity defects.

The present work investigates the dry drilling of carbon/epoxy composite (CFRE) plates. The twisted tools used are from HSS, carbide, and TiN-coated carbide, all with the same dimensions (6-mm diameter, 118° point angle, and 30° helical angle).

The effect of the cutting parameters (spindle speed and feed rate) on generated cutting forces and hole quality were studied. ANOVA was used to examine the significance and the relevance of the models used to draw the response surface in order to estimate the influence and the simultaneous interaction of the cutting parameters (rotation speed (N) and feed rate (f)) on the studied phenomena (thrust force (Fz), torque (Mz), exit delamination factor, and the cylindricity error).

2 Experimental procedure

2.1 Tests and materials

Dry drilling experiments were carried out on a CNC vertical milling machine. Three different tool materials were used for the drill: HSS,-coated carbide, and carbide, with different spindle speeds and feed rates. Experimental results were collected and recorded by a data acquisition system. The experimental conditions are summarized in Table 1.

The material used in the present investigation consisted of CFRE plates (with dimensions of $200 \times 200 \times 8$ mm^3) manufactured through hand layup of $[90°/+45°/0°/-45°]_{3s}$ under a vacuum pressure of 97 MPa. The obtained thickness of the cured plate was of 8 mm.

To check the homogeneity of the prepared composite plates and calculate the fiber volume fraction, three samples of $(10 \times 10 \times 8)$ mm^3 were cut off from different plates. The fiber content was determined by pyrolysis at a temperature of 450 °C. The obtained volume fiber fraction was equal to 67.16 % with a standard deviation estimated at 1.22 %. The mechanical properties of the material are described in Table 2.

The workpiece was mounted on a Kistler platform (9257B type) in order to measure the thrust force and the torque applied on the workpiece during the drilling process.

Geometric inside-hole defects were analyzed on a three-dimensional measuring machine (CMM) with a spherical probe of 3 mm in diameter. The measurement of the inlet and the outlet hole diameters and the cylindricity error were obtained by palpation at 24 points on the circumference of the

Table 1 Cutting conditions

Process parameters	Levels of independent parameters
Spindle speed, N (rev/min)	3000, 6000, 9000
Feed rate, f (mm/min)	60, 120, 180
Tool materials	HSS, Carbide, TiN-coated carbide

Table 2 Properties of materials (fiber and resin)

Properties of the carbon fiber	Standard grade of carbon fiber
Thickness of carbon fiber Ø (μm)	7
Tensile strength (σ) (GPa)	4.3
Young's modulus (E) (GPa)	238
Density (ρ) (g/cm^3)	1.76
Specific strength (GPa)	2.00
Epoxy resin	Epoxy SR 1710
Composite CFRE properties	
Longitudinal	Transverse
E (MPa) 127,150	8625
σ_u (MPa) 1621	36
ε_u (%) 1.3	0.4

hole at 2 mm from the upper (entry hole) and lower (exit hole) free surface, as shown in Fig. 1.

Delamination is a damage phenomenon, which occurs due to the anisotropy and brittleness of composite materials. The damage (delamination) surrounding the holes was measured using a tool maker's microscope. The exit delamination factor was calculated using the following equation:

$$Fd = \frac{D_{\max}}{d} \tag{1}$$

where the parameters F_d, D_{max}, and d are the delamination factor, the maximum diameter measured in the damaged zone, and the diameter of the drill, respectively.

The exit delamination factor was calculated at the exit side of the drill. Performance characteristics, namely thrust force, torque, exit delamination, and cylindricity error, are presented in Table 3, along with

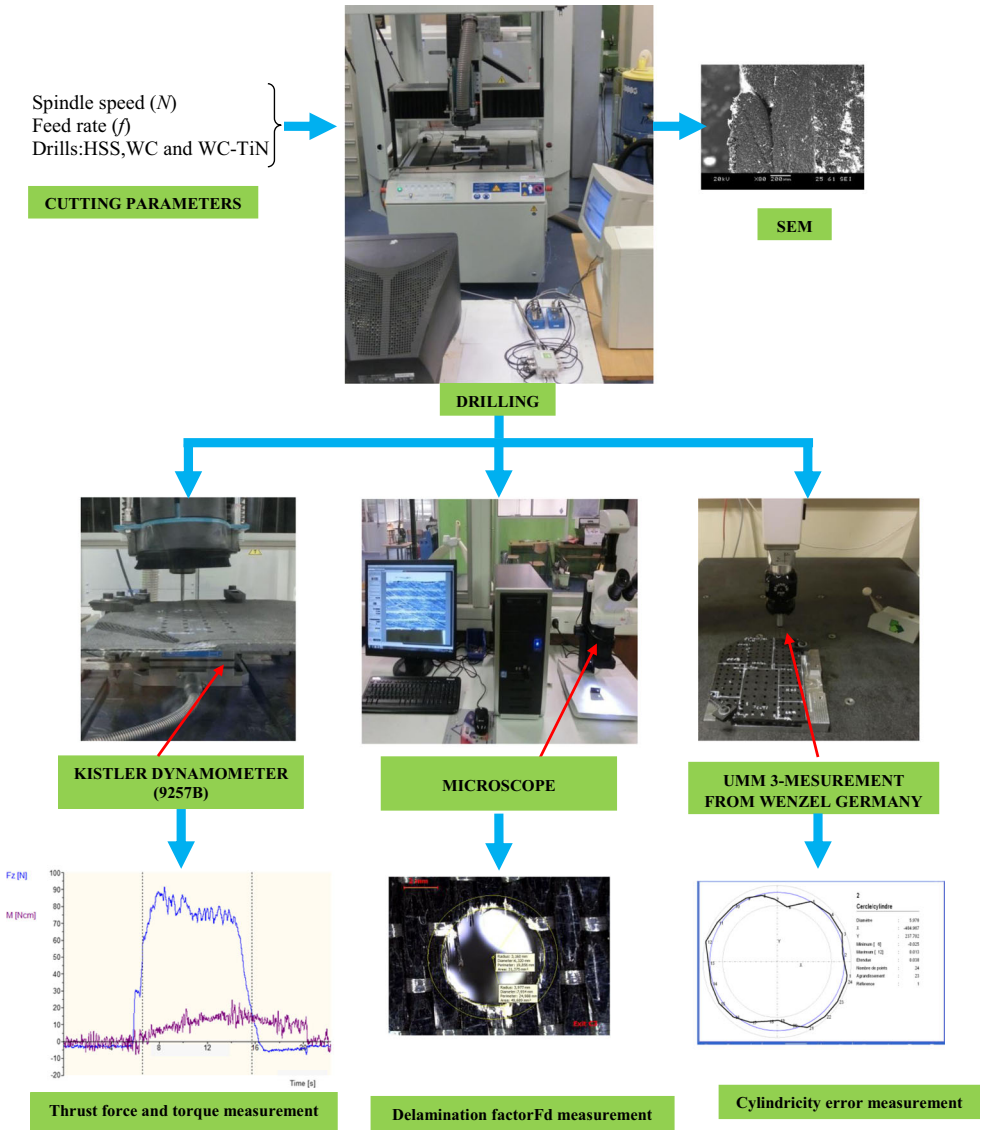

Fig. 1 Schematic of experimental processes

Table 3 Experimental results for Fz, Mz, $F_{d\text{-Exit}}$, and cylindricity error

N°	Machining parameters			Response factors			
	N (rev/min)	f (mm/s)	Drill type	Fz (N)	Mz ($N \times$ cm)	$F_{d\text{-}Exit}$ factor	Cylindricity error (mm)
1	3000	60	HSS	72.39	11.28	1.223	0.052
2	3000	60	WC	50.62	16.50	1.108	0.055
3	3000	60	WC-TiN	59.29	8.91	1.140	0.036
4	3000	120	HSS	96.69	12.90	1.355	0.042
5	3000	120	WC	62.61	23.66	1.121	0.032
6	3000	120	WC-TiN	73.15	10.17	1.142	0.025
7	3000	180	HSS	121.60	14.71	1.368	0.046
8	3000	180	WC	65.31	25.16	1.146	0.037
9	3000	180	WC-TiN	81.11	13.34	1.215	0.026
10	6000	60	HSS	50.79	16.33	1.276	0.054
11	6000	60	WC	34.42	16.51	1.118	0.070
12	6000	60	WC-TiN	39.19	12.52	1.081	0.064
13	6000	120	HSS	77.02	18.17	1.281	0.049
14	6000	120	WC	47.27	25.34	1.144	0.064
15	6000	120	WC-TiN	55.09	14.32	1.132	0.045
16	6000	180	HSS	96.68	20.71	1.347	0.050
17	6000	180	WC	53.49	27.45	1.199	0.060
18	6000	180	WC-TiN	67.03	14.67	1.183	0.039
19	9000	60	HSS	40.83	11.42	1.219	0.091
20	9000	60	WC	28.34	12.03	1.108	0.084
21	9000	60	WC-TiN	30.79	10.44	1.183	0.070
22	9000	120	HSS	30.33	11.64	1.282	0.079
23	9000	120	WC	38.78	13.02	1.134	0.064
24	9000	120	WC-TiN	44.74	10.80	1.136	0.050
25	9000	180	HSS	69.15	10.82	1.340	0.071
26	9000	180	WC	43.03	13.77	1.159	0.068
27	9000	180	WC-TiN	55.50	8.23	1.161	0.052

the input drilling parameters (spindle speed, feed rate, and tool materials).

2.2 Response surface methodology

Response surface methodology is a collection of mathematical and statistical techniques that are useful for the modeling and analysis of problems in which a response of interest is influenced by several variables and the purpose is to optimize this response [14, 18]. In our study, the response surface methodology (RSM) comprised the following six major components:

(1) Defining the independent input variables and the desired output responses.
(2) Drawing up an experimental design plan.
(3) Using response surface regression equations to find the relationship between the factors Fz, Mz, $F_{d\text{-}Exit}$, and cylindricity error by quadratic regression.
(4) Using ANOVA statistical analysis to find parameters which significantly affect the output.
(5) Obtaining the optimal set of experimental parameters that produces a maximum or minimum output value.
(6) Verifying and confirming the predicted performance characteristics by experiment.

3 Results and discussion

The machining parameters were measured according to 3^3 full factorial designs (27 experiments with actual independent process variables). The measured responses (output) are shown in Table 2. They were analyzed by Design-Expert software which indicated that quadratic models were statistically recommended.

3.1 Regression equations

RSM leads to an appropriate approximation for the true functional relationship between design parameters Y and a set of independent variables. Usually, a second-order model is used in response surface methodology [19, 20]:

$$Y = b_0 + \sum_{i=1}^{k} b_i x_i + \sum_{i=1}^{k} b_{ii} x_i^2 + \sum_{i<j}^{k} b_{ij} x_i x_j + \varepsilon \tag{2}$$

where x_i is the value of the ith machining process parameter. The terms b_0, $b_1 \ldots b_k$, and $b_{11},..,b_{kk}$ represent the regression coefficients. The residual ε indicates the experimental error. The second-order response surface Y is a function of the cutting parameters (the spindle speed N and feed rate f). The relationship between the response and the machining parameters is given by:

$$Y = b_0 + b_1 N + b_2 f + b_3 N^2 + b_4 f^2 + b_5 N \times f \tag{3}$$

where b_0, …, b_5 are the regression coefficients associated with the model.

The relationship between the design and the cutting parameters were modeled by quadratic regression. For the thrust force F_z, the models are given in Eqs. 4–6 for three different tool materials, namely carbide, high-speed steel, and TiN-coated carbide drills. Their coefficients of determination (R^2) are 95.26, 99.40, and 99.64 %, respectively.

$$\begin{aligned} Fz_{(HSS)} = {} & 75.01889 - 0.035139 \times f - 8.74444 \times 10^{-4} \\ & \times N - 2.90139 \times 10^{-5} \times f \times N + 2.00741 \\ & \times 10^{-3} \times f^2 - 3.33148 \times 10^{-7} \times N^2 \end{aligned} \tag{4}$$

$$\begin{aligned} Fz_{(WC)} = {} & 51.64333 + 0.38025 \times f - 7.87278 \times 10^{-3} \\ & \times N - 2.46716 \times 10^{-20} \times f \times N - 1.02361 \times 10^{-18} \\ & \times f^2 + 3.39444 \times 10^{-7} \times N^2 \end{aligned} \tag{5}$$

$$\begin{aligned} Fz_{(WC\cdot TiN)} = {} & 66.76667 + 0.3275 \times f - 9.94611 \times 10^{-3} \\ & \times N + 4.01389 \times 10^{-6} \times f \times N - 6.04167 \times 10^{-4} \\ & \times f^2 + 4.06667 \times 10^{-7} \times N^2 \end{aligned} \tag{6}$$

The torque (Mz) models are given in Eqs. 7 to 9. Their coefficients of determination R^2 are 96.77, 94.91, and 94.42 %.

$$\begin{aligned} Mz_{(HSS)} = {} & -11.54333 + 0.055278 \times f + 8.76 \times 10^{-3} \\ & \times N - 5.59722 \times 10^{-6} \times f \times N - 6.94444 \times 10^{-6} \\ & \times f^2 - 6.97222 \times 10^{-7} \times N^2 \end{aligned} \tag{7}$$

$$\begin{aligned} Mz_{(WC)} = {} & -12.08444 + 0.25717 \times f + 7.33889 \times 10^{-3} \\ & \times N - 9.61111 \times 10^{-6} \times f \times N - 5.84259 \times 10^{-4} \\ & \times f^2 - 6.38148 \times 10^{-7} \times N^2 \end{aligned} \tag{8}$$

$$\begin{aligned} Mz_{(WC\cdot TiN)} = {} & -8.73556 + 0.094917 \times f + 5.63833 \\ & \times 10^{-3} \times N - 9.22222 \times 10^{-6} \times f \times N - 1.14352 \\ & \times 10^{-4} \times f^2 - 3.91296 \times 10^{-7} \times N^2 \end{aligned} \tag{9}$$

The delamination-exit ($F_{d\text{-}Exit}$) factor models are shown in Eqs. 10 to 12 with coefficients of determination R^2 of 83.95, 92.32, and 79.28 %, respectively.

$$\begin{aligned} F_{d-Exit(HSS)} = {} & 1.151 + 1.83611 \times 10^{-3} \times f + 2.833 \\ & \times 10^{-6} \times N - 3.3333 \times 10^{-8} \times f \times N - 2.91667 \\ & \times 10^{-6} \times f^2 - 3.88889 \times 10^{-10} \times N^2 \end{aligned} \tag{10}$$

$$\begin{aligned} F_{d-Exit(WC)} = {} & 1.02622 - 8.05556 \times 10^{-5} \times f + 3.17222 \\ & \times 10^{-5} \times N + 1.80556 \times 10^{-8} \times f \times N + 1.85185 \\ & \times 10^{-6} \times f^2 - 2.7037 \times 10^{-9} \times N^2 \end{aligned} \tag{11}$$

$$\begin{aligned} F_{d-Exit(WC-TiN)} = {} & 1.1918 - 3.5 \times 10^{-4} \times f - 2.58889 \times 10^{-5} \\ & \times N - 1.34722 \times 10^{-7} \times f \times N + 6.62037 \times 10^{-6} \\ & \times f^2 + 3.42593 \times 10^{-9} \times N^2 \end{aligned} \tag{12}$$

The cylindricity error models are illustrated in Eqs. 13 to 15 with coefficients of determination R^2 of 98.41, 96.12, and 97.4 %, respectively.

$$\begin{aligned} \text{Cylindricty} \times \text{error}_{(HSS)} = {} & 0.07667 - 2.3333 \times 10^{-4} \\ & \times f - 8.7222 \times 10^{-6} \times N - 1.9444 \times 10^{-8} \times f \times N \\ & + 1.1111 \times 10^{-6} \times f^2 + 1.3889 \times 10^{-10} \times N^2 \end{aligned} \tag{13}$$

$$\text{Cylindricy} \times \text{error}_{(WC)} = 0.04867 - 7.3889 \times 10^{-4} \times f + 1.5444 \times 10^{-5} N + 2.7778 \times 10^{-9} \times f \times N + 2.5 \times 10^{-6} \times f^2 - 8.88889 \times 10^{-10} \times N^2 \quad (14)$$

$$\text{Cylindricty} \times \text{error}_{(WC\cdot TiN)} = 0.03211 - 6.0278 \times 10^{-4} \times f + 1.4278 \times 10^{-5} N - 1.1111 \times 10^{-8} \times f \times N + 2.17593 \times 10^{-6} \times f^2 - 6.85185 \times 10^{-10} \times N^2 \quad (15)$$

3.2 Statistical analysis

The analysis of variance (ANOVA) method consists of fractioning the total variation in an experiment into components ascribable to controlled factors and errors.

Table 4 summarizes the variant analysis results of the thrust force (Fz), torque (Mz), delamination exit factor ($F_{d\text{-}Exit}$), and cylindricity error, respectively, of composite (CFRE) drilling. This analysis was carried out for a significance level of 5 %, i.e., for a confidence level of 95 %. These tables indicate the degree of freedom DF, sum of squares SC sq., mean square MS, F values, probabilities (P value), and the percentage of contribution (Cont. %) of each factor to the total variation. At the bottom of each table, the values of the determination coefficients R^2, the adjusted R^2((Adj-R^2), the predicted R^2((Pred-R^2), and the adequate precision are given.

The analysis of the first part of Table 4 shows that the feed rate, tool, the interactions $N \times$ tool, tool × tool, and especially the spindle speed (with a contribution of 41.68 %) have a great influence on the thrust force. The interactions ($N \times f$), ($f \times$ tool), ($N \times N$), and ($f \times f$) do not present any significant contribution on the obtained thrust force. Their contributions are 0.22, 1.66, 0.08, and 0.01 %, respectively.

Furthermore, R^2 is 91.27 %, Adj-R^2 is 86.64 %, and Pred-R^2 is 78.11 %. Therefore, in this case, the value of the Pred-R^2 is in reasonable agreement with the Adj-R^2 value. Thus, the thrust force model can be used to navigate the response space. Adequate precision compares the range of predicted values at the design points to the average prediction error. It is a measure of the signal to noise ratio. A ratio greater than 4 indicates adequate model precision, and in this particular case, it was found to be 19.18, which is well above the adequate precision limit.

In the second part of Table 4, the torque (Mz) is presented. These results show that the interaction tool × tool (Cont. = 41.25 %) and interaction spindle speed $N \times N$ (Cont. = 26.88 %) have the most significant influence on the torque (Mz). However, the spindle speed (Cont. = 11.02), the feed rate (Cont. = 10.05 %), and the tool (Cont. = 5.61 %) are less significant. These results also show that $N \times f$, $N \times$ tool, $f \times f$, and $f \times$ tool interactions are negligible. The model works well in torque analysis with R^2 equal to 83.48 % which indicates a more preponderant fit of the model. The Pred-R^2 of 59.66 % is in reasonable agreement with the Adj-R^2 of 74.73 %. The signal to noise ratio obtained here is 10.37, which is well above 4 and shows an adequate signal.

It is clear from the ANOVA results that the tool is the dominant factor affecting the exit delamination factor ($F_{d\text{-}Exit}$) (third part of Table 4) with a contribution of 57.06 %. The second factor influencing $F_{d\text{-}Exit}$ is the tool × tool interaction (Cont. = 27.65). The interaction feed rate has a contribution of 14.12 %. It is the most significant parameter related to the exit delamination factor. The spindle speed N and interactions $N \times f$, $N \times$ tool, $N \times N$, $f \times f$, tool × tool, and the tool factor do not present any significant contribution to the obtained $F_{d\text{-}Exit}$. The model for surface roughness gives values of R^2, Adj-R^2, and Pred-R^2 of 92.33, 88.26, and 78.16 %, respectively. It is worth mentioning that the Pred-R^2 is in reasonable agreement with the Adj-R^2. These values should be used as indications of correctness of fit.

Finally, the results in the fourth part of Table 4 (cylindricity error) indicate that the model is still significant. Spindle speed (Cont. = 63.38 %), feed rate (Cont. = 13.23 %), cutting tool (Cont. = 13.23 %), second-order effect of tool (tool × tool) (Cont. = 4.41 %), and feed rate ($f \times f$) (Cont. = 4.27 %) are the significant terms of the model. The spindle speed is the most significant factor related to cylindricity error. This is expected because it is well known that with the increase in the spindle speed, tool vibration increases. This induces an increase in the cylindricity error [11]. The ANOVA table indicates that the interactions ($N \times f$), ($N \times$ tool), ($f \times$ tool), and ($N \times N$) do not present any significant contribution to the cutting temperature obtained (calculated value of F is more than the table value; $F_{0.05,\ 1,\ 17} = 4.45$) at 95 % confidence level. The value of R^2 is 90.10 % of the total variability, Adj-R^2 is 84.87 %, and the Pred-R^2 is 76.26 %. The latter is in reasonable agreement with the value of Adj-R^2. Adequate precision of 14.83 is an adequate value for the model to perform well in prediction.

3.3 Pareto graph

To give better view of the results of the analysis of variance, Pareto graphs were built (see Fig. 2). This figure ranks the cutting parameters and their interactions according to their growing influence on the thrust force (Fz), torque (Mz), exit delamination factor ($F_{d\text{-}Exit}$), and cylindricity error. Standardized values for this figure were obtained by dividing the effect of each factor by the error on the estimated value of the corresponding factor. If the F values were greater than 4.45, the effects were considered to be significant. Conversely, if the F value was less than 4.45, the effects were

Table 4 ANOVA result-model variation

Source	Sum of squares	DF	Mean square	*F* value	Prob.	Cont. %	R^2 %	Adj-R^2 %	Pred-R^2 %	AP
Thrust force (*Fz*)										
Model	12097.63	9	1344.18	19.74	<0.0001		91.27	86.64	78.11	19.18
N	5042.76	1	5042.76	74.05	<0.0001	41.68				
F	3368.56	1	3368.56	49.47	<0.0001	27.84				
Tool	1243.18	1	1243.18	18.26	0.0005	10.28				
N × *f*	27.00	1	27.00	0.40	0.5373	0.22				
N × tool	383.64	1	383.64	5.63	0.0297	3.17				
f × tool	200.49	1	200.49	2.94	0.1044	1.66				
N × *N*	9.21	1	9.21	0.14	0.7176	0.08				
f × *f*	1.25	1	1.25	0.018	0.8940	0.01				
Tool × tool	1821.55	1	1821.55	26.75	<0.0001	15.06				
Error	1157.67	17	68.10							
Total	13255.30	26				100				
Torque (*Mz*)										
Model	598.89	9	66.54	9.54	<0.0001		83.48	74.73	59.66	10.37
N	65.97	1	65.97	9.46	0.0068	11.02				
F	60.21	1	60.21	8.64	0.0092	10.05				
Tool	33.57	1	33.57	4.81	0.0424	5.61				
N × *f*	25.78	1	25.78	3.70	0.0714	4.30				
N × *tool*	0.35	1	0.35	0.051	0.8245	0.06				
f × *tool*	0.67	1	0.67	0.096	0.7600	0.11				
N × *N*	160.99	1	160.99	23.09	0.0002	26.88				
f × *f*	4.30	1	4.30	0.62	0.4430	0.72				
Tool × tool	247.04	1	247.04	35.43	<0.0001	41.25				
Error	118.52	17	6.97							
Total	717.42	26				100				
$F_{d\ exit}$										
Model	0.17	9	0.019	22.73	<0.0001		92.33	88.26	78.16	15.58
N	5.120E-004	1	5.120E-004	0.61	0.4470	0,30				
F	0.024	1	0.024	28.81	<0.0001	14,12				
Tool	0.097	1	0.097	114.21	<0.0001	57,06				
N × *f*	9.720E-004	1	9.720E-004	1.15	0.2985	0,57				
N × tool	6.453E-004	1	6.453E-004	0.76	0.3944	0,38				
f × tool	2.760E-003	1	2.760E-003	3.27	0.0884	1,62				
N × *N*	6.000E-006	1	6.000E-006	7.100E003	0.9338	0,00				
f × *f*	2.667E-004	1	2.667E-004	0.32	0.5816	0,16				
Tool × tool	0.047	1	0.047	55.40	<0.0001	27,65				
Error	0.014	17	8.450E-004							
Total	0.19	26				100				
Cylindricity error										
Model	6.774E-003	9	7.527E-004	17.20	<0.0001		90.10	84.87	76.26	14.83
N	4.294E-003	1	4.294E-003	98.11	<0.0001	63.38				
F	8.961E-004	1	8.961E-004	20.47	0.0003	13.23				
Tool	8.961E-004	1	8.961E-004	20.47	0.0003	13.23				
N × *f*	3.333E-005	1	3.333E-005	0.76	0.3950	0.49				
N × tool	2.133E-005	1	2.133E-005	0.49	0.4945	0.31				
f × tool	4.408E-005	1	4.408E-005	1.01	0.3296	0.65				
N × *N*	1.852E-006	1	1.852E-006	0.042	0.8395	0.03				
f × *f*	2.894E-004	1	2.894E-004	6.61	0.0198	4.27				
Tool × tool	2.987E-004	1	2.987E-004	6.82	0.0182	4.41				
Error	7.440E-004	17	4.376E-005							
Total	7.518E-003	26				100				

not considered significant. The confidence interval chosen was 95 %. *F* table corresponding to a 95 % confidence level in the accurate calculation of the process parameters was $F_{0.05,\ 1,\ 17} = 4.45$.

To verify the adequacy of the model obtained by ANOVA analysis, the normality assumption of the residual must be verified. Figure 3a, b shows normal probability plots of the residuals. These figures reveal that all the residuals follow a straight line pattern which is in good agreement with the results reported by Shahrajabian et al. [21].

4 Response surface analysis

A 3D response surface model was generated to exhibits the interaction effects due to spindle speed *N* and feed

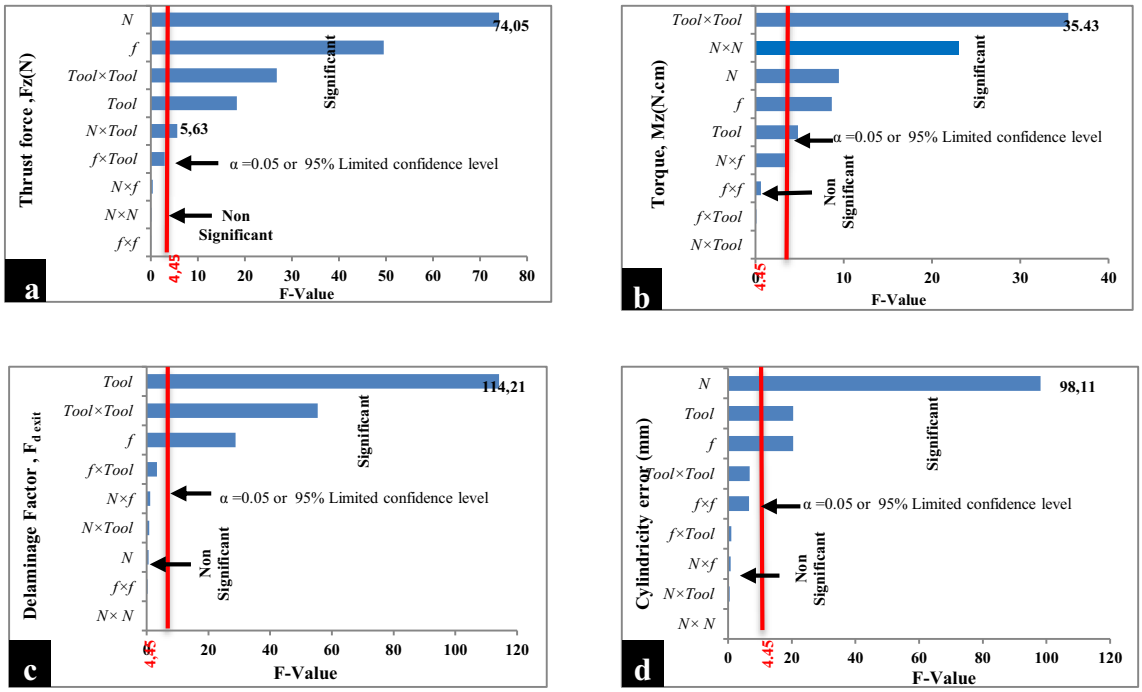

Fig. 2 Pareto graph:,**a** Thrust force, **b** torque, **c** exit delamination factor, and **d** cylindricity error

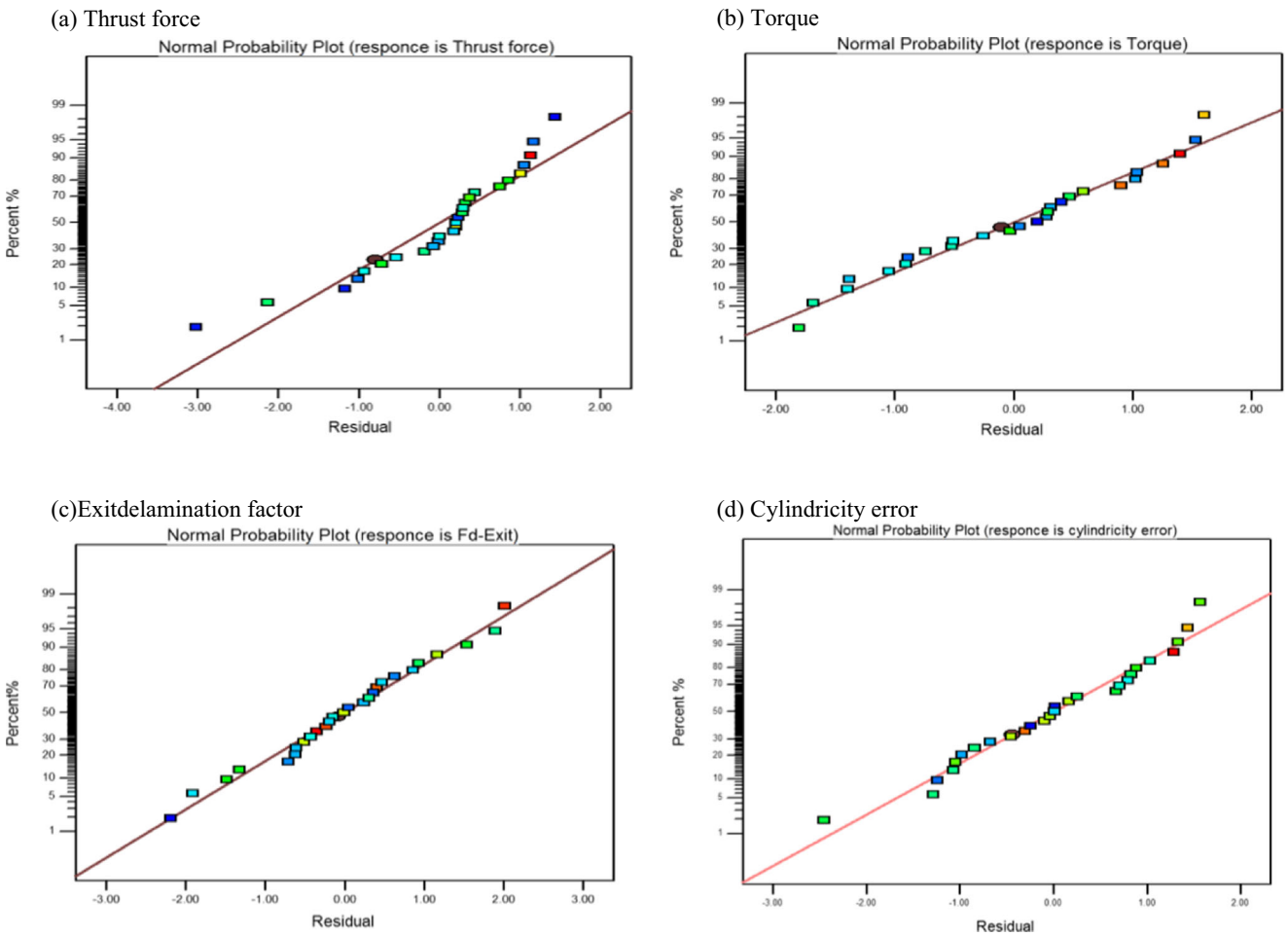

Fig. 3 Normal probability plot of residuals for each response

rate f on thrust force Fz, torque Mz, delamination factor at the exit ($F_{d\text{-}Exit}$), and the cylindricity error during drilling of CFRE composites. These were analyzed for three different drill materials: high-speed steel, carbide, and coated carbide through response surface plots (Figs. 4, 5, 6, and 7).

4.1 Effect of drilling parameters on thrust forces

The thrust force generated during drilling of CFRE composites depends on input variables, such as cutting speed or spindle speed, feed rate, and drill materials. This effect is summarized in Fig. 4. The thrust force greatly increases with the feed rate. However, the thrust force changes only slightly when the spindle speed varies. It can also be observed in this figure that drilling with the HSS drill leads to a higher thrust force compared to WC and WC-TiN drills. Furthermore, it can be noticed that for a spindle speed of 3000 rev/min with a feed rate varying from 60 to 180 mm/min, the drilling thrust force of CFRE composites using WC,WC-TiN, and HSS tools is subjected to an increase of 22.64, 26.64, and 40.47 %, respectively.

From these figures, it was noted that for the smallest feed rate (60 mm/min) and a spindle speed varying from 3000 (rev/min) to 9000 (rev/min), the thrust force for the three drills (HSS, WC, and WC-TiN) was slightly reduced. It is known that increasing the spindle speed raises the temperature of machining, which is due to the friction between the tool and the CFRE composite materials, which in turn results in a softening of the material and a subsequent reduction in thrust force [20].

4.2 Effect of drilling parameters on torque

Drilling torque obtained from the regression model and the optimum torque for the three drills (HSS, WC, and WC-TiN) is exhibited by the three-dimensional response surface model shown in Fig. 5. It can be observed that the torque increases noticeably with the feed rate for the three drilling tools. Drill materials have a significant effect on the torque during the drilling of the CFRE composites. In addition, maximal torque values are obtained when drilling composite laminates with a speed spindle of 6000 rev/min, for all three tool materials. For the same spindle speed of 6000 rev/min, the WC drill was subjected to the highest torque value when the feed rate was 180 mm/min.

Furthermore, Fig. 5 indicates that at a high spindle speed (9000 rev/min) and a low feed rate (60 mm/min), the three drills were subjected to a low torque value in the drilling of CFRE composites.

4.3 Effect of drilling parameters on the exit delamination factor

From the response surface analysis in Fig. 6, it can be seen that the exit delamination factor is highly sensitive to the feed rate variation. It can also be observed from Fig. 6 that delamination has a tendency to increase with the feed rate during drilling of CFRE composites for the different drills (HSS, WC, and WC-TiN). In addition, the HSS drill has the greatest effect on delamination compared with the other tools.

Figure 6 clearly shows that the combination of low values of feed rate and spindle speed is useful in the WC tool during drilling of CFRE composites in order to reduce damage at the

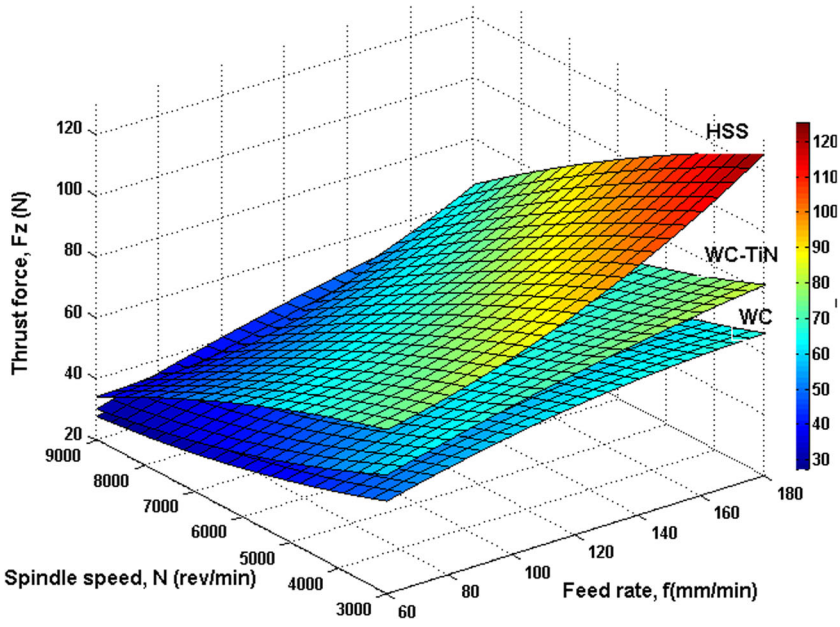

Fig. 4 Effect of spindle speed and feed rate on thrust force for HSS, carbide, and TiN-coated carbide

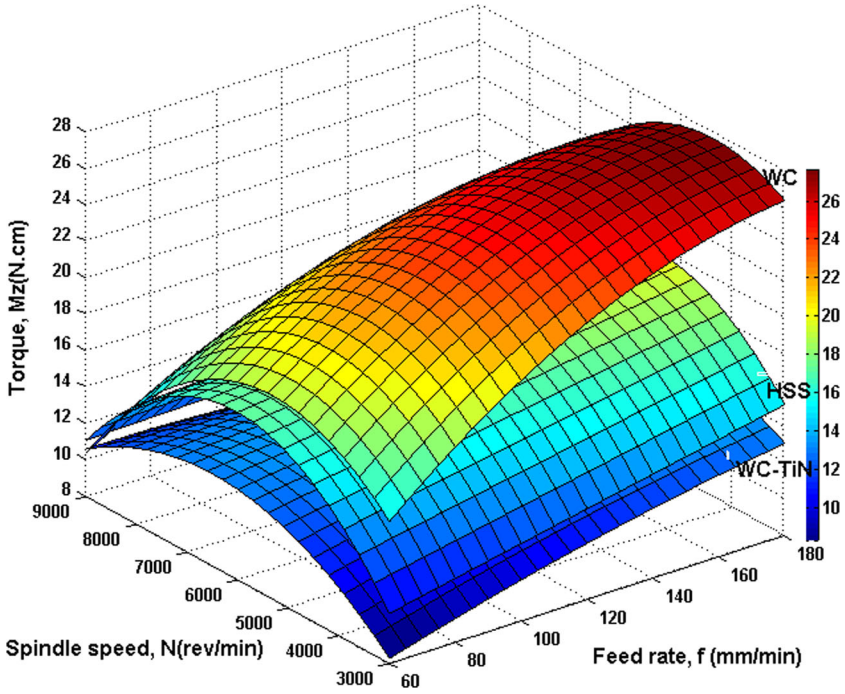

Fig. 5 Effect of spindle speed and feed rate on torque for HSS, carbide, and TiN-coated carbide

exit of the holes, and that delamination decreases with a high cutting speed (9000 rev/min).

Again according to Fig. 6, it is observed that the rise in spindle speed slightly diminishes the exit delamination factor. The reason for this is that the temperature produced in the drilling of composites increases with the spindle speed, which softens the matrix material and increases shearing, which diminishes delamination. The high feed rate increases both the thrust force in drilling and the exit delamination factor [11].

This result can be explained by the fact that at high cutting speed, the cutting edge action is reduced, and that the friction between cutting edges and board causes temperature elevation and softening, thus reducing damage.

4.4 Effect of machining parameters on cylindricity error

The influence of the feed rate and spindle speed on the cylindricity error using the HSS, WC, and WC-TiN drills is illustrated in Fig. 7. It can be observed that the cylindricity

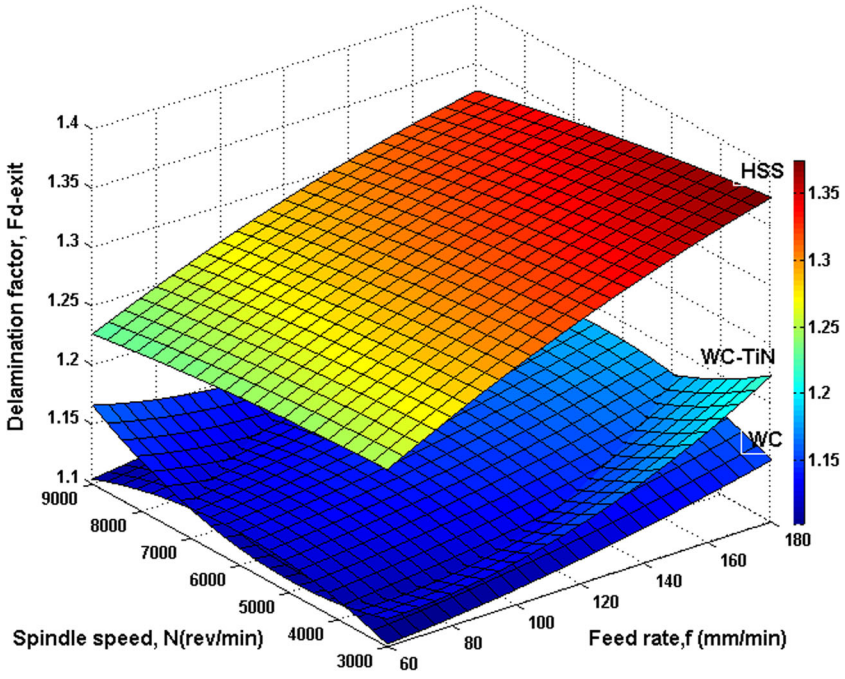

Fig. 6 Effect of spindle speed and feed rate on exite delamination factor ($F_{d\text{-exit}}$) for HSS, carbide, and TiN-coated carbide

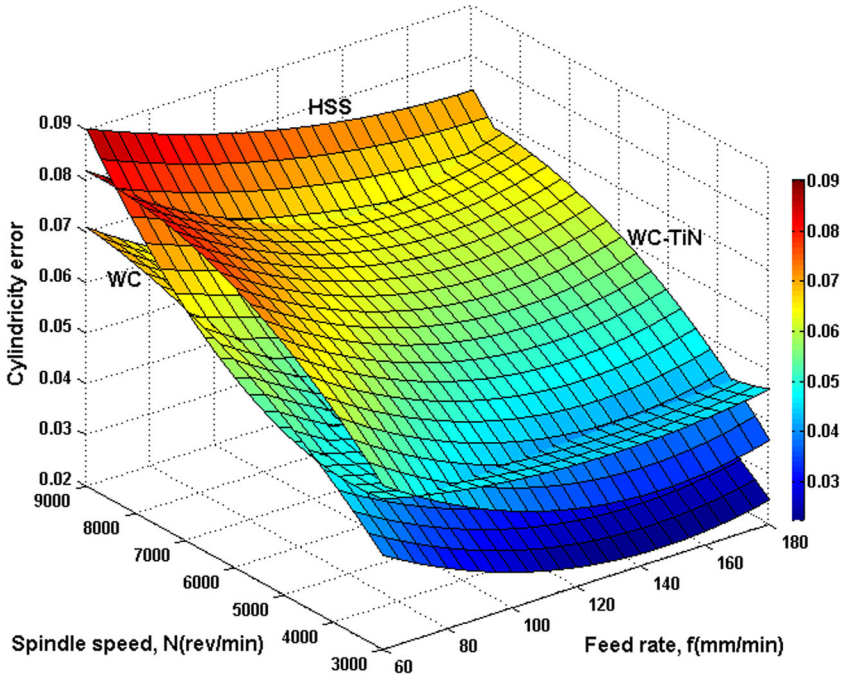

Fig. 7 Effect of spindle speed and feed rate on cylindricity error for HSS, carbide, and TiN-coated carbide

error is related linearly to both spindle speed and feed rate. The high spindle speed increases the cylindricity error in the drilling of composite materials for the different drills (HSS, WC, and WC-TiN). It is the most influential parameter on the quality of the holes, in particular the cylindricity error. On the other hand, the effect of the feed rate on the cylindricity error is insignificant for the lowest spindle speed, 3000 rev/min, and only slight for the highest spindle speed of 9000 rev/min.

It was concluded that the combination between the maximum spindle speed and the minimum feed rate for the three tools gives a maximum cylindricity error. Hence, the smallest cylindricity error is obtained from the combination of the lowest spindle speed and the highest feed rate.

5 Surface quality of machined holes

SEM observation revealed several damaged areas when the holes were machined with a WC twist drill, as shown in Fig. 8. These damaged areas were mainly observed at fiber orientations of −45° and 90°. However, in WC-Ti machining, there were fewer damage areas and lower depths of damage compared to WC drilling. Also, it was found that damage was uniformly distributed. Figure 8 displays the SEM observation of the last nine cut composite layers (90°,45°,0°,−45°, 90°, 45°, 0°, and −45°) for the holes drilled into the CFRE composite.

The SEM photograph illustrates several cases of fiber pullout and a series of interlaminar delamination damage. The extent of this damage depends mainly on the fiber orientation and the cutting parameters [22].

Observations, as illustrated in Fig. 8, show that the surface hole accumulated melted matrix material between the plies. This is possibly caused by the increased tool-workpiece contact time coupled with a low feed rate leading to relatively higher interfacial temperatures. The weak thermal conductivity of CFRE was a further contributory factor in causing the resin to melt.

A close-up view of the distribution of fibers at a 90° angle is illustrated in Fig. 8a. The material removal is initiated by an opening, which penetrates the material below the cutting direction, according to the fiber/matrix interface, extended by a secondary rupture, which rises to the shear fibers, as shown in Fig. 9a [23].

The SEM analysis also illustrates that the cutting of the fibers of plies with −45° orientation causes pullout of the

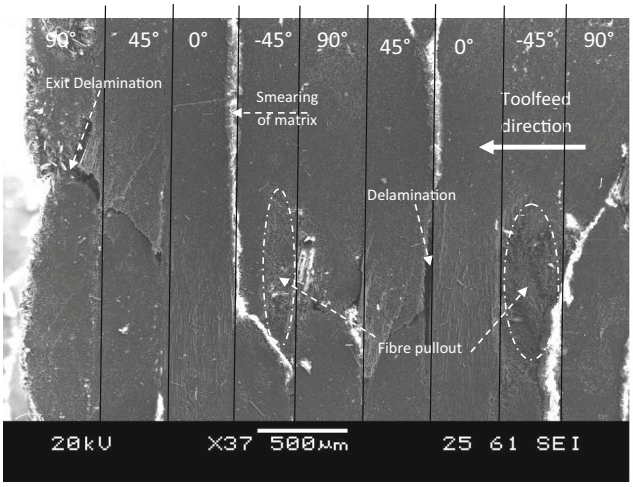

Fig. 8 SEM photographs of the damages observed of hole drilled

fibers, leading to significant damage in the form of cavities (see Fig. 8). With the cutting of −45° oriented fibers illustrated in Fig. 9b, the fibers bend. Significant defects propagate inside the material and eventually pullout and tear the fibers [24, 25].

Chip separation occurs after fiber rupture in a direction perpendicular to their axis. During the cutting of plies at 0° orientation, the tool delaminates the fibers easily creating small defects Fig. 8. Machining of fibers at 0° can produce large fragmented debris. The fibers are stressed and this induces buckling which causes cracking (Fig. 9c).

For plies of 45° orientation, the chip formation mechanisms begin with shearing of the fibers and then of the matrix, along the fiber/matrix interface to the free surface, as illustrated in Fig. 9c. During cutting of the fibers oriented at 45°, the cutting tool reached the layer directly, and very small composite debris were formed.

It can be seen that the drilling of composites produces tiny fiber particle chips, as shown in Fig. 10, with dimensions not exceeding roughly 20 μm.

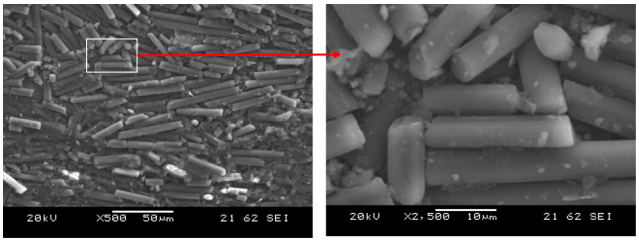

Fig. 10 SEM photographs of the CFRE chips

6 Confirmation experiments

The comparison between the expected values of the model developed in the present work (Eqs. 1 to 15) and the values obtained experimentally is shown in Table 5. It illustrates the calculated errors as follows: thrust force (Fz) (max. value 3.41 % and min. value 0.64 %), torque (Mz) (max. value 4.36 % and min. value 2.80 %), exit delamination factor ($F_{d\text{-}Exit}$) (max. value 3.20 % and min. value 0.76 %), and cylindricity error (mm) (max. value 2.82 % and min. value 1.45 %). All the confirmation experiment values are within the 95 % prediction interval. Therefore, Eqs. (1) to (15) correlated the evolution of thrust force, torque, exit delamination factor, and cylindricity error with the cutting conditions (spindle speed and feed rate) with a reasonable degree of approximation.

7 Optimization of cutting conditions

In this study, a desirability function approach was used for multiple response parameters, namely thrust force (Fz), torque (Mz), exit delamination factor ($F_{d\text{-Exit}}$), and cylindricity error. Design-Expert software was used for this optimization exercise. During the optimization process, the aim was to find the optimal values of machining parameters in order to produce the lowest thrust force, torque, surface roughness, and cutting

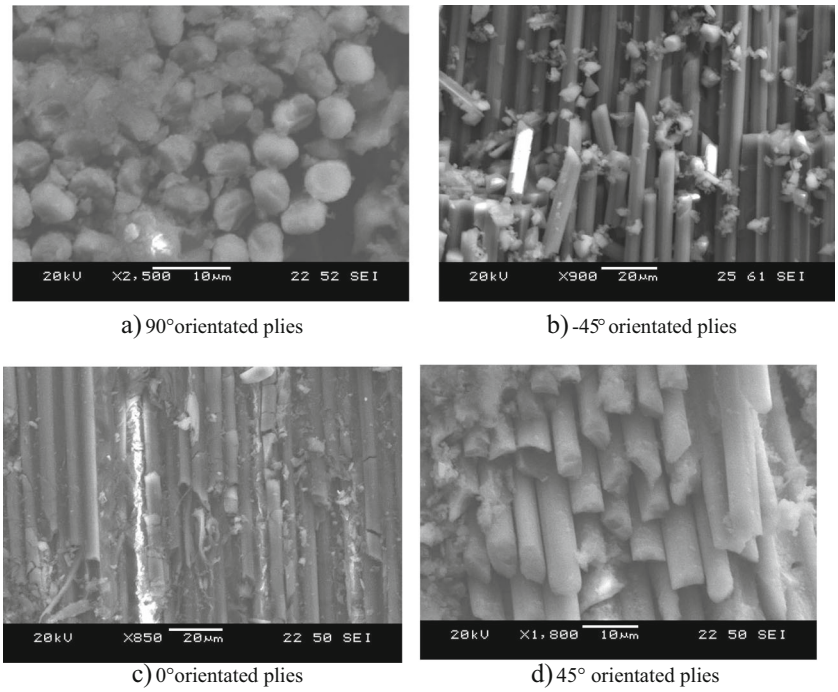

a) 90°orientated plies

b) -45° orientated plies

c) 0°orientated plies

d) 45° orientated plies

Fig. 9 SEM photographs of fracture of the hole drilled at different orientations of fiber. **a** 90° orientated plies, **b** −45° orientated plies, **c** 0° orientated plies, and **d** 45° orientated plies

Table 5 Confirmation of experiment results

Exp. N°	Design parameters			For regression equations		
	N (rev/min)	*f* (mm/min)	Tools	Exp.	Predict.	Error %
Thrust force (*Fz*)						
1	3000	180	HSS	114.32	115.06	0.64
2	3000	180	WC	73.91	76.52	3.41
3	3000	180	WC-TiN	65.08	67.27	3.25
Torque (*Mz*)						
1	3000	180	HSS	17.11	17.83	4.04
2	3000	180	WC	10.30	10.77	4.36
3	3000	180	WC-TiN	11.02	10.72	2.80
Exit delamination factor						
1	6000	180	HSS	1.29	1.25	3.20
2	6000	180	WC	1.30	1.31	0.76
3	6000	180	WC-TiN	1.17	1.18	0.85
Cylindricity error (mm)						
1	9000	60	HSS	0.073	0.071	2.82
2	9000	60	WC	0.042	0.041	2.44
3	9000	60	WC-TiN	0.068	0.069	1.45

temperature. To solve this type of parameter design problem, an objective function, $F(x)$, is defined as follows [21]:

$$DF = \left(\prod_{i=1}^{n} d_i^w\right)^{\frac{1}{\sum_{j-1}^{n} w_i}}$$
$$F(x) = -DF \tag{16}$$

with d_i the desirability defined for the ith required output and w_i the weighting of d_i.

For different objectives of required output, the desirability d_i is defined in variable forms. If an objective is to attain a particular value of Ti, the desirability d_i becomes:

$$\begin{aligned} &di = 0 \text{ if } Y_i \le \text{Low}_i \quad \text{or} \quad Y_i \ge \text{High}_i \\ &d_i = \left[\frac{Y_i - \text{Low}_i^{\,i}}{T_i - \text{Low}_i}\right] \quad \text{if} \quad \text{Low}_i \le Y_i \le T_i \\ &d_i = \left[\frac{Y_i - \text{High}_i^{\,i}}{T_i - \text{High}_i}\right] \quad \text{if} \quad T_i \le Y_i \le \text{High}_i \end{aligned} \tag{17}$$

where Yi is the value found of the ith output during the optimization process and Low_i and $High_i$ are the minimum and maximum values for the same output. If the objective is to find the maximum value, the desirability will be:

$$\begin{aligned} &di = 0 \quad \text{if} \quad Y_i \le \text{Low}_i \quad \text{or} \quad Y_i \ge \text{High}_i \\ &d_i = \left[\frac{Y_i - \text{Low}_i^{\,i}}{\text{High}_i - \text{Low}_i}\right] \quad \text{if} \quad \text{Low}_i \le Y_i \le \text{High}_i \end{aligned} \tag{18}$$

If the objective is to find a minimum value, the desirability is defined as follows:

$$\begin{aligned} &d_i = 0 \quad \text{if} \quad Y_i \le \text{Low}_i \quad \text{or} \quad Y_i \ge \text{High}_i \\ &d_i = \left[\frac{\text{High}_i - Y_i^{\,i}}{\text{High}_i - \text{Low}_i}\right] \quad \text{if} \quad \text{Low}_i \le Y_i \le \text{High}_i \end{aligned} \tag{19}$$

In Eq. (16), w_i is put as equal to one, since the d_i all have the same weight in this work. DF is a combined desirability

Table 6 Constraints for optimization of cutting conditions

Condition	Goal	Lower limit	Upper limit	Importance
Spindle speed, *N* (rev/min)	Is in range	3000	9000	
Feed rate, *f* (mm/min)	Is in range	60	180	
Tool materials	Is in range	(1) HSS, (2) WC, (3) WC-TiN		
Thrust force (*Fz*)	Minimize	28.34	121.6	****
Torque (*Mz*)	Minimize	8.23	27.45	****
Exit delamination ($F_{d\text{-Exit}}$)	Minimize	1.081	1.368	*****
Cylindricity error	Minimize	0.025	0.091	*****

Table 7 Optimization results

Solution N°	N (rev/min)	f (mm/min)	Tool materials	Fz (N)	Mz (N.cm)	$F_{d\text{-Exit}}$	Cylindricity (mm)	Desirability
1	3000	68.87	WC-TiN	58.28	8.85	1.125	0.03756	0.851
2	3000	68.19	WC-TiN	58.16	8.80	1.125	0.03778	0.851
3	3000	67.12	WC-TiN	57.98	8.72	1.125	0.03813	0.851
4	3000	71.67	WC-TiN	58.76	9.06	1.126	0.03669	0.851
5	3000	70.93	WC-TiN	58.59	9.03	1.126	0.03695	0.850
6	3000	69.78	WC-TiN	58.41	8.94	1.126	0.03731	0.850
7	3000	62.38	WC-TiN	57.17	8.35	1.123	0.03972	0.850
8	3000	61.45	WC-TiN	57.01	8.28	1.123	0.04004	0.850

function. The purpose here is to find the best solution that maximizes a combined desirability function DF, i.e., minimizes $F(x)$.

The optimal manufacturing conditions for the drilling of composite CFRE with the constraints of the cutting parametric range are those corresponding to the lowest values of thrust force (Fz), torque (Mz), exit delamination factor ($F_{d\text{-Exit}}$), and cylindricity error during the dry drilling process. The constraints used during the optimization process are summarized in Table 6, whereas the optimal solutions are reported in Table 7. This same table shows the RSM optimization results for thrust force, torque, exit delamination factor, and cylindricity error. The optimum cutting parameters in Table 7 were obtained with a spindle speed of 3000 rev/min, a feed rate of (61.45 to 71.67) mm/min, and the WC-TiN tool material. The optimized thrust force, torque, $F_{d\text{-Exit}}$, and cylindricity error are (57.01 to 58.76) N, (8.28 to 9.06) $N \times$ cm, (1.040 to 1.041), (1.123 to 1.126), and (0.03669 to 0.04004) mm, respectively.

8 Conclusions

This research work presents the application of RSM models to the study of the influence of machining parameters on thrust force, torque, exit delamination factor, and cylindricity error.

The relationship between the factors and the measured performance were modeled by quadratic regression. Three process variables, namely spindle speed, feed rate, and tool materials, were used for the development of the models. The RSM models were developed then tested using ANOVA. The actual models were found to satisfy the optimization of the machining parameters at a 95 % confidence interval. Through this analysis, conclusions about machining force, exit delamination factor, and cylindricity error were deduced:

- Drilling forces were significantly influenced by tool materials. Since the degree of drilling force induced in the drilling process is associated with the power requirements, which is in turn correlated to production costs, a low thrust force and torque were preferred. In this study, coated carbide (WC-Ti) drills induced the lowest drilling forces while HSS drills produced the highest drilling forces. Therefore, coated carbide drills present more advantages for CFRE composites drilling.
- The 3D response surface plots clearly indicate the existence of non-linear relationships between the process parameters and the machinability characteristics and thus justifying the use of a quadratic model.
- The error associated with the ANOVA table (maximum value 4.36 % and minimum value 0.64 %) for the factors and the coefficients was obtained by the quadratic regression (maximum value 92.33 % and minimum value 83.48 %).
- Comparison of experimental and predicted values of thrust force, torque, exit delamination factor, and cylindricity error shows that the good agreement has been achieved between them. Therefore, the developed model can be recommended for use in predicting thrust force, torque, exit delamination factor, and cylindricity error.
- Verification of the experiments carried out shows that the empirical models developed can be used for CRFE composites drilling.
- Hence, it is clear that a reduction in the cylindricity error for drilling composites can be achieved by using a low spindle speed and high feed rate.
- The recommended levels of the drilling parameters allowing minimal thrust force, torque, exit delamination factor, and cylindricity error simultaneously are the feed rate at level 1 (~60 mm/min), the drill type at level 3 (WC-Ti), and the spindle speed at level 1 (3000 rev/min).

Fz, thrust force (N); HSS, high-speed steel; Mz, torque ($N \times$ cm); N, spindle speed (rev/min); f, feed rate (mm/s); $F_{d\text{-Exit}}$, factor of delamination-exit.

Acknowledgments This work was completed in the Laboratory of Materials Science and Engineering (University USTHB, Algeria) in collaboration with the Laboratory of Innovative Technologies (LTI), University of Picardie Jules Verne, France). The authors would like to thank the Algerian Ministry of Higher Education and Scientific Research (MESRS) and the Delegated Ministry for Scientific Research (MDRS) for granting financial support for CNEPRU.

References

1. Chen WC (1997) Some experimental investigations in the drilling of carbon fibre reinforced composite laminations. Int J Mach Tools Manuf 37(8):1097–1108
2. Paulo Davim J, Reis P (2003) Drilling carbon fiber reinforced plastics manufactured by autoclave experimental and statistical study. Mater Des 24:315–324
3. Davim JP, Reis P (2003) Study of delamination in drilling carbon fiber reinforced plastic (CFRP) using design experiments. Compos Struct 59:481–487
4. Tsao CC (2008) Experimental study of drilling composite materials with step-core drill. Mater Des 29:1740–1744
5. Zitoune R, El M, Krishnaraj V (2013) Tribo-functional design of double cone drill implications in tool wear during drilling of copper mesh/CFRP/woven ply. Wear 302:1560–1567
6. Lia MJ, Sooa SL, Aspinwalla DK, Pearsonb D, Leahyc W (2014) Influence of lay-up configuration and feed rate on surface integrity when drilling carbon fibre reinforced plastic (CFRP) composites. Procedia CIRP 13:399–404
7. Gaitonde VN, Karnik SR, Rubio Campos J, Correia Esteves A, Abrao AM, Paulo Davim J (2008) Analysis of parametric influence on delamination in high-speed drilling of carbon fiber reinforced plastic composites. J Mater Process Technol 203:431–438
8. Rawat S, Attia H (2009) Characterization of the dry high speed drilling process of woven composites using machinability maps approach. CIRP Annals ManufTechnol 58:105–108
9. Piquet R, Ferret B, Lachaud F, Swider P (2000) Experimental analysis of drilling damage in thin carbon/epoxy plate using special drills. Compos Part A 31:1107–1115
10. Durão LMP, Tavares JMRS, de Albuquerque VHC, Gonçalves DJS (2013) Damage evaluation of drilled carbon/epoxy laminates based on area assessment methods. Compos Struct 96:576–583
11. Capello E (2004) Workpiece damping and its effect on delamination damage in drilling thin composite laminates. J Mater Process Technol 148:186–195
12. Bhatnagar N, Ramakrishnan N, Naik NK, Komanduri R (1995) On the machining of fiber reinforced plastic (FRP) composite laminates. Int J Mach Tools Manuf 35:701–716
13. Rajamurugan TV, Shanmugam K, Palanikumar K (2013) Analysis of delamination in drilling glass fiber reinforced polyester composites. Mater Des 45:80–87
14. Khashaba UA, EI-Sobaty IA, Selmy AI, Megahed AA (2010) Machinability analysis in drilling woven GFR/epoxy composites: part I—effect of machining parameters. Compos Part A 41: 391–400
15. Rubio Juan Carlos C, Rubio JCC, da Silva LJ, de Oliveira Leite Tulio Hallak Panzera W, Sergio Luiz Moni Ribeiro F, João Paulo D (2013) Investigations on the drilling process of unreinforced and reinforced polyamides using Taguchi method Composites. Part B Eng 55:338–344
16. Sardinas RQ, Reis P, Davim JP (2006) Multi-objective optimization of cutting parameters for drilling laminate composite materials by using genetic algorithms. Compos Sci Technol 66:3083–3088
17. Krishnamoorthy A, Rajendra Boopathy S, Palanikumar K, Paulo Davim J (2012) Application of grey fuzzy logic for the optimization of drilling parameters for CFRP composites with multiple performance characteristics. Measurement 45:1286–1296
18. DeFuLiu YJT, Cong WL (2012) A review of mechanical drilling for composite laminates. Compos Struct 94:1265–1279
19. Aouici H, Bouchelaghem H, Yallese MA, Elbah M, Fnides B (2014) Machinability investigation in hard turning of AISI D3 cold work steel with ceramic tool using response surface methodology. Int J Adv Manuf Technol 73:1775–1788
20. Haijin W, Jie S, Jianfeng L, Laixiao L, Nan L (2016) Evaluation of cutting force and cutting temperature in milling carbon fiber-reinforced polymer composites. Int J Adv Manuf Technol 82(9): 1517–1525
21. Shahrajabian H, Farahnakian M (2013) Modeling and multi-constrained optimization in drilling process of carbon fiber reinforced epoxy composite. Int J Precis Eng Manuf 14:1829–1837
22. Rubio JCC, Abrao AM, Faria PE (2008) Delamination in high speed drilling of carbon fiber reinforced plastic (CFRP). J Compos Mater 42(15):1523–1532
23. Sahraie Jahromi A, Bahr B, Krishnan KK (2014) An analytical method for predicting damage zone in orthogonal machining of unidirectional composites. J Compos Mater 48(27):3355–3365
24. Zhenchao Q, Kaifu Z, Hui C, Dong W, Qingxun M (2015) Microscopic mechanism based force prediction in orthogonal cutting of unidirectional CFRP. Int J Adv Manuf Technol 79:1209–1219
25. Cadorin N, Zitoune R, Seitier P, Collombet F (2015) Analysis of damage mechanism and tool wear while drilling of 3D woven composite materials using internal and external cutting fluid. J Compos Mater 49(22):2687–2703